

REGISTRATION OF IMAGES WITH TOPOLOGICAL CHANGE VIA RIEMANNIAN EMBEDDING

Xiaoxing Li[†] Xiaojing Long* Christopher Wyatt* *the Alzheimer's Disease Neuroimaging Initiative*

[†]GE Global Research, One Research Circle, Niskayuna, NY, 12309

*Department of Electrical and Computer Engineering, Virginia Tech, Blacksburg, VA, 24061

ABSTRACT

In this paper, we develop a new deformable registration algorithm for images with pathology-induced topological changes. In this algorithm, 3D images are embedded as 4D surfaces in a Riemannian space and the registration is conducted as a surface evolution process. Our algorithm differs from existing methods in the sense that it takes an *a-priori* estimation of areas with topological change as an additional input and generates dense deformation vector fields which are free of false deformation. In particular, the output of our algorithm is composed of a diffeomorphic deformation field and an intensity displacement which corrects the intensity difference caused by the topological changes. The experiments demonstrate that our proposed algorithm is capable of accurately registering images with considerable topological changes. More importantly, the resulting deformation field is not impacted by topological changes, i.e., there is no false deformation.

Index Terms— deformable registration, topological change, false deformation, Riemannian embedding, brain MRI.

1. INTRODUCTION

Deformable registration has been found to have the potential of picking up detailed structural differences among imaged subjects, and thus has triggered great research interest [1, 2, 3]. It is well known that brain diseases such as multiple sclerosis (MS) and leukoaraiosis can alter the intensity in brain magnetic resonance image (MRI). This in turn changes the topology of the image level-sets. Such *topological changes* can cause *false deformation* in the resulting dense vector fields of existing deformable registration algorithms [4]. Consequently, in the subsequent analysis such as deformation-based morphometry (DBM) that relies on the

Some of the data used in the preparation of this article were obtained from the Alzheimer's Disease Neuroimaging Initiative (ADNI) database (www.loni.ucla.edu/ADNI). As such, the investigators within the ADNI contributed to the design and implementation of ADNI and/or provided data but did not participate in analysis or writing of this report. ADNI investigators include (complete listing available at www.loni.ucla.edu/ADNI/Collaboration/ADNI_Authorship_list.pdf).

dense vector fields, false deformation will be wrongly associated with local growth or shrinkage [5]. To handle this, existing DBM works include an additional step of removing lesions via in-painting prior to performing registration [5]. However, these works require a reasonably accurate segmentation of lesions and a possibly sophisticated in-painting algorithm. Another approach is the metamorphosis theory [6]. A metamorphosis is a Riemannian metric defined on the space of images to account for both geometric deformation and intensity changes. Metamorphosis has been used in facial morphing and medical image averaging [7]. However, in metamorphosis, input images are set to be the base points of the deformation. Then, topological changes will impact both spatial deformation and intensity displacement in the registration process. As a result, false deformation is still expected to be present. In more recent work [8], 2D images are also registered in a Riemannian space, although topological changes are not particularly modeled in the registration process.

Alternatively, some registration algorithms use pathology models to handle topological changes [9]. However, the pre-computed model is limited to that specific pathology, e.g., a certain type of tumor. Note that brain resections or the presence of neurosurgical instruments can also be regarded as topological changes in general. In those applications, methods are developed to register brain images with resections by matching subvolumes [10] or landmarks [11]. The work by Risholm et. al. [11] uses anisotropic diffusion instead of Gaussian smoothing in a Demons registration framework and generates a deformation field that is free of the impact from resections. However, when handling scattered lesions, such as in case of MS, this approach need to model each lesion-affected region as a separate diffusion sink, which will induce a heavy computational load to the registration process. Note that, in this work bias and noise are not regarded as topological changes and thus are not particularly modeled.

In our previous work, we developed a registration algorithm via embedding images into higher dimensional Riemannian space [12, 13]. The algorithm was used to register 2D images without specifically suppressing false deformation. In this work, however, we develop a new registration method to handle topological changes by suppressing their impact on

the deformable registration process for brain MRI. Specifically, images in \mathbf{R}^3 Euclidian space are embedded as surfaces in an \mathbf{R}^4 Riemannian space. The registration process is then conducted as surface deformation, where the first three dimensions of the resulting deformation field correspond to the spatial grid deformation in the \mathbf{R}^3 Euclidian space, and the 4th dimension corresponds to the intensity displacement. Compared with metamorphosis, our embedding models the two types of deformation in a metamorphosis, i.e., a spatial deformation and a template evolution, with a single partial differential equation (PDE) evolution in a higher dimensional space. This guarantees a smooth convergence of the diffusion to a local minimum. In addition, by carefully choosing a feature-space in the embedding, we are able to control the distribution of the deformation energy in a way that topological changes are mainly attributed to intensity displacement, while brain structural changes are mostly captured by a diffeomorphism of spatial grid deformation. In doing so, topological changes will not impact the spatial deformation and thus false deformation is effectively suppressed.

2. REGISTRATION ALGORITHM

Our algorithm is derived from the Sochen-Kimmel-Malladi general non-linear diffusion [1], by choosing a particular embedding for our specific problem. The surface evolution follows the Euler-Lagrange equation that minimizes the surface weight measured by the Polyakov functional. Specifically, an image manifold (Σ, g) in \mathbf{R}^3 is embedded as an \mathbf{R}^4 feature-space manifold (M, h) , where g and h are the metric tensors on Σ and M , respectively. The map $X : \Sigma \rightarrow M$ is chosen as

$$X = [x, y, z, I(x, y, z)], \quad (1)$$

where x, y, z are the local image Cartesian coordinates in \mathbf{R}^3 , and $I(x, y, z)$ is the intensity of the pixel at (x, y, z) . Based on this map X and a metric h , the metric g is determined through the pullback procedure as the following,

$$g_{\mu\nu} = h_{ij} \partial_\mu X^i \partial_\nu X^j. \quad (2)$$

Note that (2) uses Einstein summation convention, with $\mu, \nu \in \{x, y, z\}$, $i, j \in \{x, y, z, I\}$ in our embedding. The summation convention will be used in all our equations from now on. In (2), $g_{\mu\nu}$ represents the (μ, ν) th element of g and h_{ij} stands for the (i, j) th element of h .

Using the above definitions, the weight of the map $X : \Sigma \rightarrow M$ is calculated as:

$$S[X^i, g_{\mu\nu}, h_{ij}] = \int d^m \sigma \sqrt{g} g^{\mu\nu} \partial_\mu X^i \partial_\nu X^j h_{ij}, \quad (3)$$

where $g^{\mu\nu}$ is the (μ, ν) element of g^{-1} , \sqrt{g} is the square root of the metric g 's determinant, and m is the dimension of Σ . This equation is referred to as the Polyakov functional in

Riemannian geometry. The variation of the Polyakov functional with respect to the embedding can be found by the Euler-Lagrange equation. This variation defines the gradient descent direction that minimizes the Polyakov functional, following which the embedded surface shrinks its area most rapidly, until it completely vanishes. It has been shown that many image processing tasks can be accomplished via minimizing the Polyakov functional, e.g., image smoothing and segmentation [1].

In the same spirit, we conduct registration via the minimization of the Polyakov Functional. We define the metric h in the following form,

$$h = \begin{bmatrix} \phi & 0 & 0 & 0 \\ 0 & \phi & 0 & 0 \\ 0 & 0 & \phi & 0 \\ 0 & 0 & 0 & \beta\phi \end{bmatrix}, \quad (4)$$

where ϕ is a positive function that influences the shape of a harmonic map, i.e., change the physical meaning of a minimal weight of the surface. ϕ provides us with the flexibility of adjusting the path of diffusion, similar to the geodesic surfaces [14], and enables the minimal surface flow to achieve the desired objective. β defines the feature-space of the embedding, which is the relative magnitude between feature and space, i.e., image intensity and image spatial Cartesian grid. We choose $\phi = (I_m - I_f)^2$, where I_m and I_f are the moving and the fixed (target) images, respectively. ϕ is a function used to adjust the area of embedded surface. When the moving and the fixed images are perfectly aligned, ϕ will have zero-value everywhere and the surface area measured by the Polyakov functional will achieve its minimal value, zero. β is a factor that defines the relative magnitude between feature and space. The choice of β impacts the distribution of deformation energy. If we have a function $p(x, y, z)$, whose value indicates the probability that the pixel at (x, y, z) lies within a topological change, we can construct the function β in the following form,

$$\beta(x, y, z) = \frac{1}{p(x, y, z) + \epsilon}, \quad (5)$$

where ϵ is a small positive value to avoid the ill-condition of division-by-zero. With this function, for image regions without topological change, $p(x, y, z)$ will have small values and β will have large values accordingly. Then the deformation in these regions will mainly concentrate on spatial grid to capture the structural difference between the moving and the target images. On the other hand, for image regions that do have topological change, $p(x, y, z)$ will have large values and β will thus have small values. Then intensity displacement will be favored during the registration process to correct the appearance of topological change in these regions. In our applications, we choose to use a Gaussian blurred binary lesion segmentation label map as $p(x, y, z)$.

Using the map given in (1) and the chosen h in (4), we can obtain the metric g through the pullback procedure in (2). Then, the gradient direction that minimizes surface area is given by the Euler-Lagrange equation. We take the gradient descent approach and derive the equation for surface variation as the following,

$$\frac{\partial X}{\partial t} = \frac{\phi^2}{\sqrt{g}} \partial_\mu (\sqrt{g} g^{\mu\nu} \partial_\nu X^k) + \phi^2 \Gamma_{ij}^k \partial_\mu X^i \partial_\nu X^j g^{\mu\nu}. \quad (6)$$

Here, t is the time variable that represents discrete step in the diffusion process. Note that in (6), the Euler-Lagrange equation is multiplied by ϕ^2 which is a positive function and will not affect the solution of the minimization. In addition, Γ_{ij}^k , $k, i, j \in \{x, y, z, I\}$ are the elements in the Levi-Civita connection, given by

$$\Gamma_{jk}^i = \frac{1}{2} h^{il} (\partial_j h_{lk} + \partial_k h_{jl} - \partial_l h_{jk}). \quad (7)$$

Combining the above definitions and after several mathematical manipulations, we can obtain the following registration updating rule:

$$\frac{\partial X}{\partial t} = S_1 \begin{bmatrix} -\beta I_x \\ -\beta I_y \\ -\beta I_z \\ 1 \end{bmatrix} + S_2 \begin{bmatrix} I_x \\ I_y \\ I_z \\ I_x^2 + I_y^2 + I_z^2 \end{bmatrix} + S_3 \begin{bmatrix} -\beta I_x \\ -\beta I_y \\ -\beta I_z \\ 1 \end{bmatrix}, \quad (8)$$

where,

$$\begin{aligned} S_1 &= \frac{\phi}{\kappa^2} [(1+\beta I_y^2 + \beta I_z^2) I_{xx} + (1+\beta I_x^2 + \beta I_z^2) I_{yy} + (1+\beta I_x^2 + \beta I_y^2) I_{zz}] \\ &\quad - \frac{2\phi\beta}{\kappa^2} (I_x I_y I_{xy} + I_x I_z I_{xz} + I_y I_z I_{yz}) \\ &\quad + \frac{3}{2\kappa} (\phi_x \beta I_x + \phi_y \beta I_y + \phi_z \beta I_z - \phi_I) \\ S_2 &= -\frac{\phi I}{2\kappa}, \\ S_3 &= -\frac{\phi}{2\kappa\beta} (\beta_x I_x + \beta_y I_y + \beta_z I_z) (1 + \kappa), \\ \kappa &= 1 + \beta I_x^2 + \beta I_y^2 + \beta I_z^2, \end{aligned}$$

where the subscripts all denote partial derivatives.

For medical image registration, certain regularizations play crucial role to ensure a physically meaningful registration result. Most state-of-the-art registration algorithms constrain the resulting deformation field to be in the group of diffeomorphisms [2, 3]. A subtle difference in our registration is that, only the first three dimensions of the surface evolution represent spatial grid change, and thus are required to be diffeomorphic. The 4th dimension, however, is the intensity displacement that is expected to capture high frequency variations and should not be confined in the group of diffeomorphisms. Clearly, in our method, adding explicit constraints only to the first three dimensions of the deformation is mathematically difficult. Instead, as proposed in

diffeomorphic demons [3], spatial deformation can be directly performed in the Lie group of diffeomorphisms. Thus, the registration results are diffeomorphic when the Lie algebra is applied during the optimization, avoiding the typical routine of adding constraints into the objective. Following this idea, we adopt the *intrinsic updating rule*:

$$s \leftarrow s \circ \exp(u) \quad (9)$$

for the evolution of the spatial deformation field. Here, s is the vector field of the overall spatial deformation and u contains the first three components of the surface evolution (8): $u = [\frac{\partial X^1}{\partial t}, \frac{\partial X^2}{\partial t}, \frac{\partial X^3}{\partial t}]^T$. $\exp(\ast)$ stands for the vector field exponential operation, which can be efficiently computed through iterative composition [3]. The intensity displacement, on the other hand, is directly accumulated as follows

$$\Delta \leftarrow \Delta + \delta, \quad (10)$$

where Δ is the overall intensity displacement, and δ is the last component of the surface evolution (8): $\delta = \frac{\partial X^4}{\partial t}$. After applying intensity displacement Δ on the target image I_f :

$$I_f = I_f + \Delta, \quad (11)$$

the intensity difference caused by topological changes will be eliminated. As a result, we refer to this step as *intensity correction*.

3. EXPERIMENTS AND RESULTS

3.1. Registration of image with lesions.

In the first experiment, we take the MRI of a healthy subject from OASIS dataset [15] as the moving image, as shown in the first row in Fig. 1. The target image is set to be the MRI of an alzheimers patient from ADNI dataset¹, as shown in the second row in Fig. 1. The lesions in the target image are segmented using the FreeSurfer tool [16] (segmented with the label *white matter hypointensity lesion*), and marked out using blue contours. The image of healthy subject is affine registered to the target images before applying our deformable registration algorithm. During the registration process, image L_2 residual stops dropping and starts oscillating around 85th iteration, thus the process is terminated after 100 iterations.

¹(<http://www.loni.ucla.edu/ADNI>). The ADNI was launched in 2003 by the National Institute on Aging (NIA), the National Institute of Biomedical Imaging and Bioengineering (NIBIB), the Food and Drug Administration (FDA), private pharmaceutical companies and non-profit organizations, as a \$60 million, 5-year public-private partnership. The primary goal of ADNI has been to test whether serial magnetic resonance imaging (MRI), positron emission tomography (PET), other biological markers, and clinical and neuropsychological assessment can be combined to measure the progression of mild cognitive impairment (MCI) and early Alzheimer's disease (AD). Determination of sensitive and specific markers of very early AD progression is intended to aid researchers and clinicians to develop new treatments and monitor their effectiveness, as well as lessen the time and cost of clinical trials.

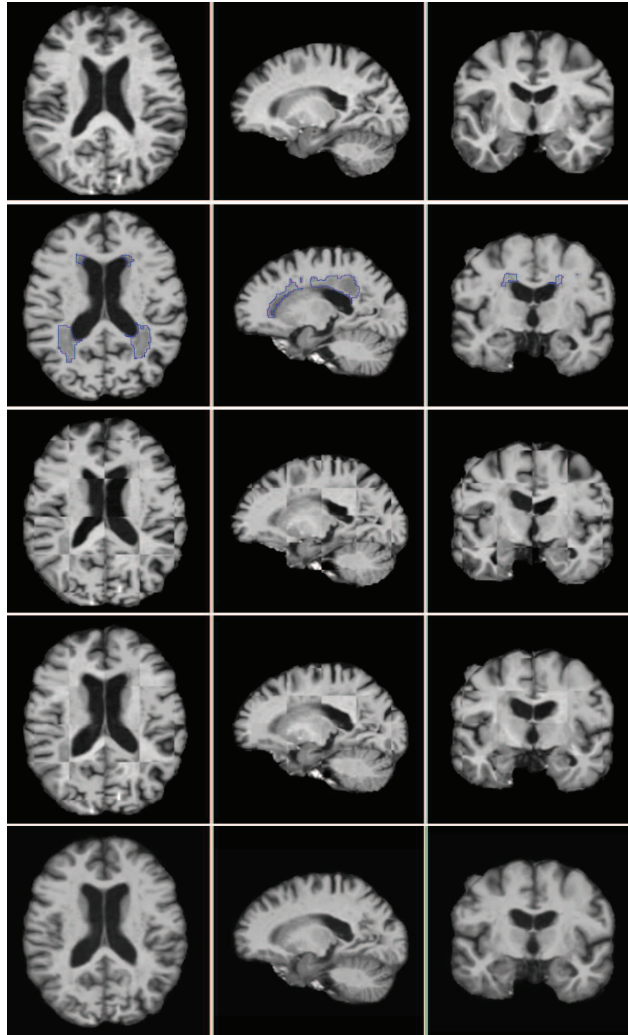


Fig. 1. Register MRI of a healthy subject to that of a patient with lesion.

The checkerboard image of the moving and target image before our deformable registration is shown in the third row of Fig. 1. The fourth row in Fig. 1 gives the checkerboard image of the target image and the registered moving image, i.e., after spatial deformation is applied. In the fifth row of Fig. 1, we show the intensity corrected target image, after intensity displacement is applied. In Fig. 1 we can see that the anatomical structures in the template are well aligned with those on the target images and the intensity within lesions in the target image is corrected to become the same as healthy white matter.

In addition, the curves plotting the L_2 image residual during the registration process are shown in Fig. 2, where the solid line plots the image L_2 residual after the spatial deformation field of the current iteration is applied to the moving image, and the dashed line plots image L_2 residual after the

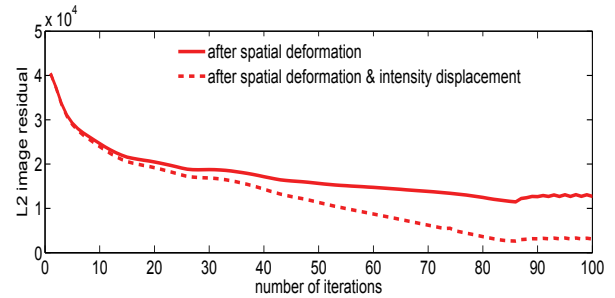


Fig. 2. Curves plotting the registration residual during the registration process.

intensity displacement is *additionally* applied. From these curves, we observe a smooth diffusion process both on the evolution of spatial deformation and on that of the intensity displacement.

For comparison purposes, the diffeomorphic demons algorithm [3] is used to perform the same registration experiment. Fig. 3 show the registration results using our proposed algorithm and diffeomorphic demons. In Fig. 3, the left and the right figure in the first row show the axial views of the moving image and the target image, respectively. The registered moving image (after spatial deformation) using our algorithm (left), and using diffeomorphic demons (right) are shown in the second row. We find that the diffeomorphic demons algorithm tries to deform the lateral ventricle into the white matter with lesions, which leads to a wrong registration result. In contrast, these errors are not seen in our registration results. The third row of Fig. 3 shows the glyph view of the deformation field obtained using our method (left) and diffeomorphic demons (right) in a zoomed region. From the vector field obtained by diffeomorphic demons, we can observe a dense deformation energy concentration (abnormally long vectors) around the lesion-affected areas, which is obviously false deformation. On the other hand, such false deformation is successfully removed in the results obtained using our algorithm. We need to emphasize that, despite the advantages of our algorithm shown by these results, keep in mind that our algorithm does take lesion segmentation as an additional input which is important prior knowledge.

3.2. Registration of image with meningioma.

In this experiment, we register a brain MR image template, as shown in the first row of Fig. 4, to a target image that carries a brain tumor of considerable size, as shown in the second row of Fig. 4. The template image was constructed using 233 healthy young subjects (mean age 34.58) from OASIS dataset in our previous study [17]. The brain image with tumor was taken for a patient with meningioma and is available in the testing data distributed within the Slicer3 [18] package. It was skull-stripped using FSL (BET) tool[19]. As shown in

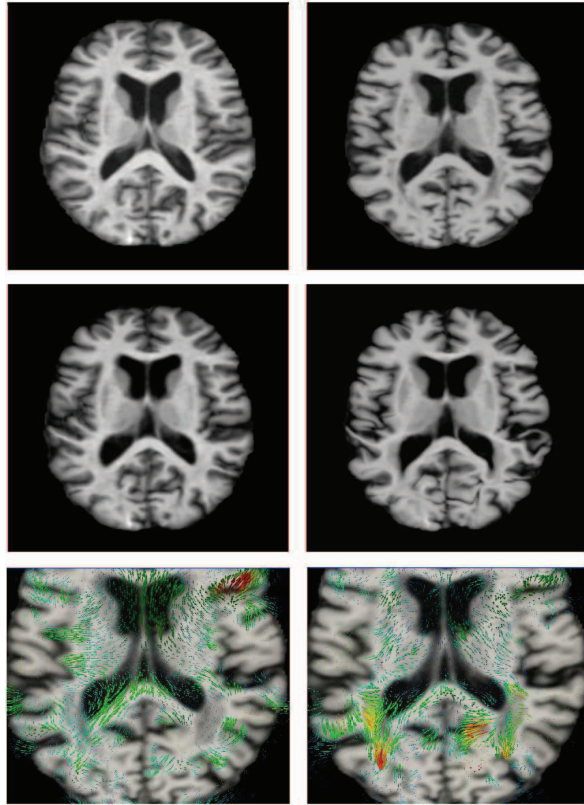


Fig. 3. Comparison of deformation fields obtained using our algorithm and diffeomorphic demons.

the second row of Fig. 4, instead of a precise segmentation of the tumor, our interface allows a physician to draw 3 profile lines on the target image to indicate the location and size of the tumor (with orange line), which gives us an ellipsoid containing the tumor region (blue contours).²

The third row of Fig. 4 gives the checkerboard image of the target image and the template; where the fourth row gives the checkerboard image of the target images and the registered template, after applying spatial deformation. We find that after registration, the template is well aligned with the target image. The fifth row shows the target image after applying intensity displacement, where we see the intensity of the tumor region is replaced by that of the co-aligned tem-

²Note that in the checkerboard images in the third and fourth rows, the target image appears to be much darker compared to the template. The appearances of the target image before and after intensity correction, as shown in the second and fifth rows, are also very different. This is due to the fact that the target image has a very different intensity profile because of the bright tumor. As a result, the contrast of the whole image is not good, where CSF appears to be dark and not really visible. However, if we pay some close attention, it is easy to notice that major features, such as the separation between gray matter and white matter and the boundary of ventricle are all well aligned after the deformable registration. Also, as shown in the fifth row, after the intensity of the tumor region is repaired, brain regions other than the tumor can be visualized with a proper intensity contrast.

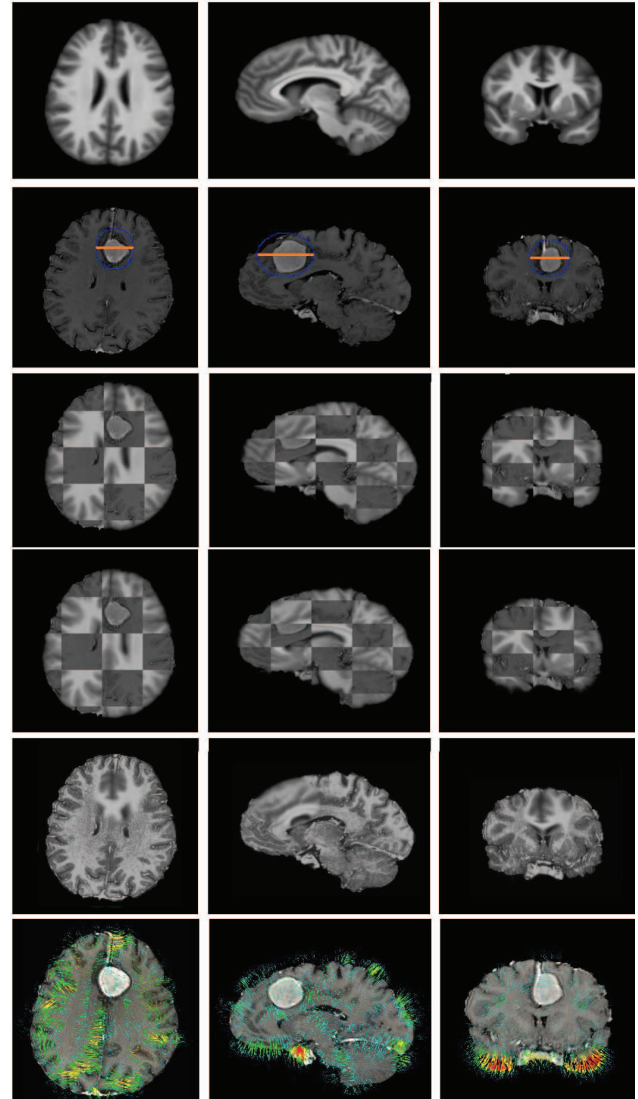


Fig. 4. Register a brain template to the MRI of a meningioma patient.

plate image. This step essentially provides us with a “tumor-repaired” version of the target image, which is an estimation of the brain anatomy had the tumor not existed. We notice that in the target image, the growth of tumor pushes the surrounding tissue aside and squeezes the ventricle. After intensity correction, the healthy tissue is moved back to the normal location and the ventricle is lifted. In the sixth row, we plot the resulting deformation field using glyphs. Clearly, the tumor does not induce any false deformation, despite the strong intensity gradient between the tumor region and the surrounding healthy tissue. In view of these results, we believe that the proposed algorithm might also be used to register images of resections.

4. CONCLUSION

In this work, we present a new deformable registration algorithm for images with topological changes. The registration is performed by embedding images in \mathbf{R}^3 Euclidian space into surfaces in an \mathbf{R}^4 Riemannian space. Then the image registration is modeled as a surface evolution process. The registration results demonstrate the efficacy of our proposed algorithm in terms of converging to correct registration in the presence of lesion.

5. REFERENCES

- [1] N. Sochen R. Kimmel and R. Malladi, "From high energy physics to low level vision," *Scale-Space Theory in Computer Vision, Lecture Notes in Computer Science*, vol. 1252, pp. 236–247, 1997.
- [2] M. F. Beg, M. I. Miller, A. Trounev, and L. Younes, "Computing large deformation metric mappings via geodesic flows of diffeomorphisms," *International Journal of Computer Vision*, vol. 61, no. 2, pp. 139–157, 2005.
- [3] T. Vercauteren, X. Pennec, A. Perchant, and N. Ayache, "Non-parametric diffeomorphic image registration with the demons algorithm," in *MICCAI Lecture Notes in Computer Science*, 2007, vol. 4792, pp. 319–326.
- [4] X. Li and C.L. Wyatt, "Modeling topological changes in deformable registration," in *ISBI'10: Proceedings of the 2010 IEEE international conference on Biomedical imaging*, 2010, pp. 360–363.
- [5] M. Sdika and D. Pelletier, "Nonrigid registration of multiple sclerosis brain images using lesion inpainting for morphometry or lesion mapping," *Human Brain Mapping*, vol. 30(4), pp. 1060–1067, 2009.
- [6] A. Trounev and L. Younes, "Metamorphoses through lie group action," *Foundations of Computational Mathematics*, vol. 5(2), 2005.
- [7] T. Hartkens, D. L. G. Hill, A. D. Castellano-Smith, D. J. Hawkes, C. R. Maurer, A. J. Martin, W. A. Hall, H. Liu, and C. L. Truweit, "Using points and surfaces to improve voxel-based non-rigid registration," *Lecture Notes in Computer Science*, vol. 2489, pp. 565–572, 2002.
- [8] D. Zosso, X. Bresson, and J.P. Thiran, "Geodesic active fields - a geometric framework for image registration," *IEEE Transaction on Image Processing*, Nov. 18, 2010. [preprint].
- [9] E.I. Zacharaki, C.S. Hogeand, D. Shen, G. Biros, and C. Davatzikos, "Non-diffeomorphic registration of brain tumor images by simulating tissue loss and tumor growth," *Neuroimage*, vol. 46, pp. 762–774, 2009.
- [10] O. Clatz, H. Delingette, I.-F. Talos, A.J. Golby, R. Kikinis, F.A. Jolesz, N. Ayache, and S.K. Warfield, "Robust nonrigid registration to capture brain shift from intraoperative mri," *IEEE Transactions on Medical Imaging*, vol. 24, no. 11, pp. 1417–1427, nov. 2005.
- [11] P. Risholm, E. Samset, and III W.M. Wells, "Validation of a non-rigid registration framework that accommodates tissue resection," in *SPIE*, 2010.
- [12] C.L. Wyatt and P. J. Laurienti, "Nonrigid registration of images with different topologies using embedded maps," in *Proceedings of IEEE Engineering in Medicine and Biology Conference*, 2006.
- [13] C.L. Wyatt, X. Li, and X. Gong, "A framework for registration of images with varying topology using embedded maps: Riemannian embedding spaces," in *BSL Report BSL2009-0001, Bioimaging Systems Laboratory, Department of Electrical and Computer Engineering Virginia Polytechnic Institute and State University*, 2009.
- [14] A. Yezzi, S. Kichenassamy, A. Kumar, P. Olver, and A. Tannenbaum, "A geometric snake model for segmentation of medical imagery," *IEEE Trans. on Medical Imaging*, vol. 16, pp. 199–209, 1997.
- [15] D. Marcus, T. Wang, J. Parker, J. Csernansky, J. Morris, and R. Buckner, "Open access series of imaging studies (oasis): cross-sectional mri data in young, middle aged, nondemented, and demented older adults," *Journal of Cognitive Neuroscience*, vol. 19, pp. 1498–1507, 2007.
- [16] A. Dale, B. Fischl, and M. Sereno, "Cortical surface-based analysis i: Segmentation and surface reconstruction," *NeuroImage*, vol. 9(2), pp. 179–194, 1999.
- [17] X. Long and C.L. Wyatt, "Structural template formation with discovery of subclasses," in *Proc. SPIE*, 2010.
- [18] "<http://www.slicer.org/>," .
- [19] S. Smith, P. R. Bannister, C. Beckmann, J. M. Brady, S. Clare, D. Flitney, P. Hansen, M. Jenkinson, D. Leiboivici, B. Ripley, M. Woolrich, and Y. Zhang, "Fsl: New tools for functional and structural brain image analysis," *NeuroImage*, vol. 13, 2001.